ULTRA SONO GRAPHY

Characterization of non-alcoholic fatty liver disease–related hepatocellular carcinoma on contrast-enhanced ultrasound with Sonazoid

Yi Dong[1], Juan Cheng[1], Yun-Lin Huang[1], Yi-Jie Qiu[1], Jia-Ying Cao[1], Xiu-Yun Lu[1], Wen-Ping Wang[2], Kathleen Möller[3], Christoph F. Dietrich[1,4]

[1]Department of Ultrasound, Xinhua Hospital Affiliated to Shanghai Jiao Tong University School of Medicine, Shanghai, China; [2]Department of Ultrasound, Zhongshan Hospital, Fudan University, Shanghai, China; [3]Medical Department I/Gastroenterology, SANA Hospital Lichtenberg, Berlin, Germany; [4]Department Allgemeine Innere Medizin, Kliniken Hirslanden, Beau Site, Salem and Permanence, Bern, Switzerland

Purpose: This study aimed to evaluate the contrast-enhanced ultrasound with Sonazoid (Sonazoid-CEUS) features of hepatocellular carcinoma (HCC) in patients with non-alcoholic fatty liver disease (NAFLD).

Methods: In this retrospective study, patients who underwent surgical resection and were histopathologically diagnosed with NAFLD or cirrhosis-related HCC were included. All patients received Sonazoid-CEUS examinations within 1 week prior to hepatic surgery. The enhancement patterns of HCC lesions were evaluated and compared between the two groups according to the current World Federation for Ultrasound in Medicine and Biology guidelines. Multivariate logistic regression analysis was used to assess the correlations between Sonazoid-CEUS enhancement patterns and clinicopathologic characteristics.

Results: From March 2022 to April 2023, a total of 151 patients with HCC were included, comprising 72 with NAFLD-related HCC and 79 with hepatitis B virus (HBV) cirrhosis–related HCC. On Sonazoid-CEUS, more than half of the NAFLD-related HCCs exhibited relatively early and mild washout within 60 seconds (54.2%, 39/72), whereas most HBV cirrhosis–related HCCs displayed washout between 60 and 120 seconds (46.8%, 37/79) or after 120 seconds (39.2%, 31/79) (P<0.001). In the patients with NAFLD-related HCC, multivariate analysis revealed that international normalized ratio (odds ratio [OR], 0.002; 95% confidence interval [CI], 0.000 to 0.899; P=0.046) and poor tumor differentiation (OR, 21.930; 95% CI, 1.960 to 245.319; P=0.012) were significantly associated with washout occurring within 60 seconds.

Conclusion: Characteristic Sonazoid-CEUS features are useful for diagnosing HCC in patients with NAFLD.

Keywords: Non-alcoholic fatty liver disease; Hepatocellular carcinoma; Contrast-enhanced ultrasound; Sonazoid; Kupffer phase

Key points: Characteristic enhancement patterns of non-alcoholic fatty liver disease (NAFLD)–related hepatocellular carcinoma (HCC) on contrast-enhanced ultrasound with Sonazoid (Sonazoid-CEUS) were identified. These patterns include hyperenhancement during the arterial phase followed by relatively early washout. Sonazoid-CEUS features of NAFLD-related HCC exhibit associations with international normalized ratio, tumor differentiation, and hepatic steatosis grade.

ORIGINAL ARTICLE

https://doi.org/10.14366/usg.24205
eISSN: 2288-5943
Ultrasonography 2025;44:232-242

Received: November 15, 2024
Revised: March 5, 2025
Accepted: March 13, 2025

Correspondence to:
Christoph F. Dietrich, MD, PhD, MBA, Department Allgemeine Innere Medizin, Kliniken Hirslanden, Beau Site, Salem and Permanence, Schänzlihalde 11, Bern, 3036, Switzerland

Tel, Fax. +41-31-337-7984
E-mail: c.f.dietrich@googlemail.com

How to cite this article:
Dong Y, Cheng J, Huang YL, Qiu YJ, Cao JY, Lu XY, et al. Characterization of non-alcoholic fatty liver disease–related hepatocellular carcinoma on contrast-enhanced ultrasound with Sonazoid. Ultrasonography. 2025 May;44(3):232-242.

Introduction

Non-alcoholic fatty liver disease (NAFLD) is the leading chronic liver disease worldwide. Its more advanced subtype, non-alcoholic steatohepatitis (NASH), is characterized by progressive liver injury that can lead to cirrhosis and hepatocellular carcinoma (HCC) [1,2]. NAFLD is the most rapidly increasing cause of HCC, paralleling the rise in obesity and diabetes in the general population [3]. Due to the growing obesity pandemic, the high prevalence of NAFLD is increasingly contributing to the overall incidence of NAFLD-related HCC in non-cirrhotic livers [2]. Cirrhosis is a well-known and significant risk factor for NAFLD-related HCC. However, NAFLD-related HCC can also develop in patients without cirrhosis, unlike liver diseases of other etiologies such as alcohol-related and autoimmune liver disease [4]. Approximately 20% to 30% of cases of NAFLD-related HCC occur in the absence of advanced fibrosis [5]. An understanding of the imaging characteristics of NAFLD-related HCC compared to those of HCC of other etiologies could aid in improving the imaging diagnosis of HCC, which is paramount for establishing more appropriate treatment strategies. Urgent measures to increase global awareness and identify high-risk populations for surveillance programs are necessary to reduce the impending burden of NAFLD-related HCC.

Ultrasound is the first-line imaging method for screening patients with clinical suspicion of NAFLD, as it is readily available and facilitates superior disease-specific surveillance [6]. Conventional B-mode ultrasound (BMUS) has a reported sensitivity of 85% and a specificity of 95% for detecting moderate to severe steatosis, although it lacks accuracy in evaluating mild steatosis [7,8]. However, BMUS has shown only 43% to 54% sensitivity and 22% to 43% specificity in accurately characterizing focal liver lesions (FLLs) [9–11]. Multiple studies have highlighted that patients with NAFLD or obesity are at higher risk for severe visualization limitations on BMUS scans compared to those with cirrhosis of other etiologies and should be considered for alternative treatment strategies [12–14].

With the injection of contrast agents, contrast-enhanced ultrasound (CEUS) improves the accurate diagnosis of FLLs [6]. Fat accumulation is the primary factor leading to vascular impairment and increased vascular resistance. CEUS can be used to assess the hepatic microcirculation and quantify early changes in parenchymal flow before the onset of fibrosis [15]. Furthermore, CEUS features may relate to prognostic factors of HCC lesions, such as tumor differentiation, microvascular invasion (MVI), pathological subtype, and Ki-67 expression level [16]. With advances in imaging techniques, CEUS holds promise for bridging the gap between medical imaging and personalized medicine. The contrast agent Sonazoid is taken up by Kupffer cells in the liver mononuclear macrophage system, producing a unique Kupffer phase on CEUS [17]. This distinct phase of CEUS with Sonazoid (Sonazoid-CEUS) allows for an extended evaluation period of up to 10 minutes to assess the washout features of FLLs [18]. However, limited information is available regarding the Sonazoid-CEUS features of NAFLD-related HCCs.

The aim of this study was to investigate the Sonazoid-CEUS characteristics of histopathologically confirmed NAFLD-related HCCs compared with those of hepatitis B virus (HBV) cirrhosis–related HCCs.

Materials and Methods

Compliance with Ethical Standards

This retrospective observational study received institutional review board approval from the authors' university hospital (ID: B2020-424R). The requirement for informed consent was waived. All aspects of the study were performed in accordance with the Declaration of Helsinki.

Patients

Patients diagnosed with HCC in the context of NAFLD or HBV-related liver cirrhosis, based on surgical resection and histopathological findings, at the university hospital were retrospectively included and analyzed. The inclusion criteria were as follows: (1) adult patients aged 18 to 85 years; (2) patients with FLLs that were clearly detectable on BMUS and who underwent Sonazoid-CEUS within 1 week before hepatic surgery; (3) patients who received surgical resection and obtained a histopathological diagnosis for both the FLLs and the adjacent liver parenchyma; and (4) patients diagnosed with NAFLD or HBV-related liver cirrhosis. The exclusion criteria were as follows: (1) patients with fatty liver caused by alcohol or other known factors; (2) patients who received other treatments, such as neoadjuvant radiotherapy and/or chemotherapy, local ablative therapy, or transarterial therapy, before surgery; and (3) liver transplantation recipients.

Baseline characteristics of the patients were collected, specifically: (1) demographic data; (2) metabolic factors, including body mass index (BMI), hypertension, diabetes, and hyperlipidemia; (3) blood profile, including platelets, international normalized ratio (INR), total bilirubin, direct bilirubin, albumin, alanine transaminase, aspartate transaminase, alkaline phosphatase, gamma-glutamyl transferase, total cholesterol, triglyceride (TG), high-density lipoprotein, and low-density lipoprotein; and (4) tumor markers, including alpha-fetoprotein, alpha-fetoprotein-L3, protein induced by vitamin K absence or antagonist-II, and microRNA.

Ultrasound Examination Technique

BMUS and Sonazoid-CEUS examinations were performed for all patients by two radiologists with more than 20 years of experience in liver CEUS, who were aware of the patients' clinical histories. All ultrasound examinations were conducted using two premium ultrasound systems: the Acuson Sequoia unit (5C1 convex array probes, 3.5 MHz; Siemens Healthineers, Mountain View, CA, USA) and the Resona R9 Super (SC6-1U convex array probes, 1–6 MHz; Mindray, Shenzhen, GD, China). A standardized Sonazoid-CEUS protocol was used as recently described in a series of articles regarding the characterization of FLLs [19,20]. First, a BMUS scan was performed to locate the suspected HCC lesions. Subsequently, 0.6 mL of Sonazoid contrast agent (perflubutane microbubbles, GE Healthcare, Oslo, Norway) was injected via a 20-gauge intravenous catheter placed in the cubital vein, immediately followed by a 5-mL saline flush. CEUS was performed using contrast harmonic real-time imaging at a mechanical index of 0.18–0.22. Each examination lasted at least 30 minutes after the injection of Sonazoid, and all examinations were digitally recorded for subsequent analysis.

Imaging Analysis

All ultrasound images were reviewed by two independent radiologists who were unaware of the patients' clinical histories, other imaging findings, and the final pathological diagnosis. On BMUS, the ultrasound criteria evaluated included location, size, echogenicity (hyperechoic, hypoechoic, or mixed echoic), margin (well- or ill-defined), shape (regular or irregular), and color Doppler flow imaging (CDFI) features of the FLLs. In patients with multiple lesions, only the largest was evaluated for the study. In accordance with current World Federation for Ultrasound in Medicine and Biology (WFUMB) guidelines, the FLLs were characterized during the following four phases on Sonazoid-CEUS: arterial phase (10–45 seconds), portal venous phase (45–120 seconds), late phase (2–8 minutes), and Kupffer phase (>8 minutes) [21]. The evaluated imaging features included enhancement degree during the arterial phase (hyperenhancement, hypoenhancement, or isoenhancement relative to the surrounding liver parenchyma), necrosis (the presence of non-enhancing areas during the arterial phase), enhancement patterns during the late phase (isoenhancement or hypoenhancement), time of washout (<60 seconds, 60–120 seconds, or >120 seconds), and degree of washout (mild or marked) [21].

Histopathological Analysis

The histopathological examination was performed in consensus by two pathologists with more than 15 years of experience who were blinded to the clinical information and imaging findings. Resected liver specimens were fixed in 10% neutral formalin or Bouin fixative, embedded in paraffin, and sectioned at 4 μm for hematoxylin-eosin and Masson trichrome staining. Non-tumoral liver parenchyma was assessed at a sufficient distance from the tumor to avoid inflammatory and fibrotic changes associated with tumor proximity. Tumor differentiation was classified as well, moderate, or poor. Hepatic steatosis was graded as S0 (steatosis in <5% of hepatocytes), S1 (5%–33%), S2 (34%–66%), and S3 (>66%) according to the Kleiner scoring system [15]. NAFLD was defined by the presence of hepatic fat in ≥5% of hepatocytes. Hepatic fibrosis was staged as F0 (no fibrosis), F1 (portal fibrosis without septa), F2 (portal fibrosis with rare septa), F3 (numerous septa without cirrhosis), and F4 (cirrhosis), while hepatic inflammation activity was evaluated as A0 (no activity), A1 (mild), A2 (moderate), and A3 (severe) according to the METAVIR scoring system [22]. MVI was defined as the presence of tumor emboli in the central vein, portal vein, or large capsular vessels under microscopy. MVI was evaluated as M0 (absent), M1 (mild positive), or M2 (moderate positive). The Ki-67 level was also reported.

Statistical Analysis

All statistical analyses were performed using SPSS Statistics version 20.0 (IBM Corp., Armonk, NY, USA) and GraphPad Prism 8 (GraphPad Software Inc., San Diego, CA, USA). Categorical variables were expressed as frequencies and proportions and compared between groups using the chi-square test or Fisher exact test. Continuous variables were first tested for normality, then reported as mean±standard deviation for normally distributed data or as median with interquartile range for non-normally distributed data. The Student t-test or Mann-Whitney U test was utilized as appropriate. Univariate and multivariate logistic regression analyses were used to assess the correlations between clinicopathologic characteristics and Sonazoid-CEUS enhancement patterns. A P-value of less than 0.05 was considered to indicate statistical significance.

Results

Baseline Characteristics

From March 2022 to April 2023, a total of 151 patients (32 female and 119 male; mean age, 58.9±11.0 years) who were histopathologically diagnosed with HCC were retrospectively included. Based on the histopathological evaluation of the liver parenchyma, patients were divided into two groups: NAFLD-related HCC (n=72) and HBV cirrhosis–related HCC (n=79). The baseline characteristics of the patients are presented in Table 1.

Table 1. Baseline characteristics of the 151 patients included

Characteristic	NAFLD-related HCC (n=72)	HBV cirrhosis–related HCC (n=79)	P-value
Demographic data			
Age (year)	59.0±10.6	58.8±11.4	0.916
Sex (male/female)	58/14	61/18	0.616
Metabolic factors			
BMI (kg/m^2)	26.0±3.1	23.3±3.1	<0.001
Hypertension	29 (40.3)	27 (34.2)	0.438
Diabetes	13 (18.1)	14 (17.7)	0.957
Hyperlipidemia	21 (29.2)	6 (7.6)	0.001
Biochemical profile			
PLT (×10^9/L)	161.0 (115.0–201.8)	127.0 (105.0–159.0)	0.005
INR	1.04 (1.00–1.12)	1.09 (1.04–1.13)	0.012
TBil (μmol/L)	13.1 (9.5–17.3)	11.9 (9.6–15.1)	0.562
DBil (μmol/L)	3.7 (2.6–5.1)	3.8 (2.8–5.4)	0.541
ALB (g/L)	42.6±2.9	41.1±3.5	0.004
ALT (U/L)	25.5 (20.0–41.0)	25.0 (17.0–37.0)	0.441
AST (U/L)	23.0 (19.0–32.0)	26.0 (20.0–41.0)	0.371
ALP (U/L)	78.5 (65.3–95.8)	82.0 (66.0–110.0)	0.207
GGT (U/L)	33.5 (26.0–68.0)	33.0 (23.0–73.0)	0.236
TC (mmol/L)	4.19±0.85	3.92±0.87	0.055
TG (mmol/L)	1.30 (0.94–1.64)	0.98 (0.71–1.19)	<0.001
HDL (mmol/L)	1.05 (0.87–1.20)	1.10 (0.95–1.33)	0.054
LDL (mmol/L)	2.50±0.75	2.27±0.75	0.063
Tumor markers			
AFP (ng/mL)	6.6 (2.7–57.8)	67.9 (2.7–653.0)	0.052
AFP-L3 (%)	3.8 (0.5–18.4)	8.9 (0.5–29.7)	0.053
PIVKA-II (mAU/mL)	107.0 (34.0–1,176.5)	144.0 (32.0–2,154.0)	0.478
microRNA	−0.09±0.57	0.12±0.66	0.045

NAFLD, non-alcoholic fatty liver disease; HCC, hepatocellular carcinoma; HBV, hepatitis B virus; BMI, body mass index; PLT, platelets; INR, international normalized ratio; TBil, total bilirubin; DBil, direct bilirubin; ALB, albumin; ALT, alanine transaminase; AST, aspartate transaminase; ALP, alkaline phosphatase; GGT, gamma-glutamyl transferase; TC, total cholesterol; TG, triglyceride; HDL, high-density lipoprotein; LDL, low-density lipoprotein; AFP, alpha-fetoprotein; AFP-L3, alpha-fetoprotein-L3; PIVKA-II, protein induced by vitamin K absence or antagonist-II.

Histopathological Findings

Among the 72 patients with NAFLD-related HCC, the liver parenchyma exhibited a histologic steatosis grade of S1 (mild steatosis) in 35 (48.6%) patients, S2 (moderate steatosis) in 19 (26.4%), and S3 (severe steatosis) in 18 (25.0%). In terms of fibrosis stage, 11 (15.3%) patients had grade F0, four (5.6%) had grade F1, 24 (33.3%) had grade F2, and 33 (45.8%) had grade F3.

A significant difference in hepatic inflammation activity was observed between the two groups (P=0.004). Furthermore, the Ki-67 level was significantly higher in patients with cirrhosis than in those with NAFLD (P=0.019). No significant differences were found in tumor differentiation or MVI (P>0.05).

Conventional Ultrasound Features

The mean size of the NAFLD-related HCC lesions was 36.6±19.8 mm. On BMUS, most lesions were heterogeneous and predominantly hypoechoic (68.1%, 49/72), with ill-defined margins and irregular shape.

Color flow signals were detected in 59.7% (43/72) of the NAFLD-related HCC lesions in non-cirrhotic livers. Spectral Doppler trace analysis revealed a mean resistance index (RI) of 0.67±0.10. No significant differences were observed in the size, location, echogenicity, CDFI features, or RI values of HCC lesions between the two groups.

Table 2. Features of HCCs on contrast-enhanced ultrasound with Sonazoid

Characteristic	NAFLD-related HCC (n=72)	HBV cirrhosis–related HCC (n=79)	P-value
Enhancement pattern during AP			>0.99
Hyperenhancement	66 (91.7)	72 (91.1)	
Homogeneous hyperenhancement	2 (2.8)	2 (2.5)	
Rim-like hyperenhancement	0	1 (1.3)	
Isoenhancement	4 (5.6)	4 (5.1)	
Time of washout			<0.001
<60 seconds	39 (54.2)	11 (13.9)	
60–120 seconds	21 (29.2)	37 (46.8)	
>120 seconds	12 (16.7)	31 (39.2)	
Degree of washout			0.634
Mild	41 (56.9)	48 (60.8)	
Marked	31 (43.1)	31 (39.2)	
Enhancement pattern during LP			
Isoenhancement	3 (4.2)	10 (12.7)	
Hypoenhancement	69 (95.8)	69 (87.3)	
Presence of non-enhanced necrosis	6 (8.3)	6 (7.6)	0.867

Values are presented as number (%).
HCC, hepatocellular carcinoma; NAFLD, non-alcoholic fatty liver disease; HBV, hepatitis B virus; AP, arterial phase; LP, late phase.

Sonazoid-Enhanced CEUS Features

After intravenous injection of Sonazoid, most of the NAFLD-related HCC lesions (91.7%, 66/72) exhibited complete hyperenhancement during the arterial phase. No significant differences were observed in arterial phase enhancement patterns between the two groups (P>0.05).

During the portal venous phase, approximately half of the NAFLD-related HCC lesions displayed relatively early and mild washout before 60 seconds (54.2%, 39/72) (Fig. 1). In contrast, most cirrhosis-related HCC lesions demonstrated mild washout between 60 and 120 seconds (46.8%, 37/79) or after 120 seconds (39.2%, 31/79) (P<0.001) (Fig. 2). However, no significant differences were found in the degree of washout between the two groups (P>0.05).

During the late phase, most NAFLD-related HCC lesions displayed hypoenhancement (95.8%, 69/72) compared with the surrounding liver parenchyma, while three (4.2%, 3/72) exhibited isoenhancement. No significant differences were observed in late phase enhancement patterns between the two groups (P>0.05).

Subsequently, all HCC lesions demonstrated hypoenhancement during the Kupffer phase (100.0%, 72/72). The Sonazoid-CEUS features are presented in Table 2.

Correlation between Clinicopathologic Characteristics and Washout Patterns

The influence of clinicopathologic characteristics on washout patterns is detailed in Table 3. In the univariate analysis, INR, high-density lipoprotein level, and tumor differentiation (moderate and poor) were associated with a washout time of less than 60 seconds in NAFLD-related HCC (P=0.018, P=0.036, P=0.045, and P=0.006, respectively). However, in the multivariate logistic regression analysis, only INR (odds ratio [OR], 0.002; 95% confidence interval [CI], 0.000 to 0.899; P=0.046) and poor tumor differentiation (OR, 21.930; 95% CI, 1.960 to 245.319; P=0.012) remained significantly associated.

Discussion

Due to its advantages for long-term imaging and the high stability of Sonazoid microbubbles, clinicians can obtain more diagnostic information with Sonazoid-CEUS than with other modalities [23]. This retrospective study reports the Sonazoid-CEUS findings and clinicopathologic data from 72 patients with NAFLD-related, surgically treated HCC compared with 79 patients with cirrhosis-related HCC.

Regarding clinical and laboratory data, the patients with HCC and NAFLD exhibited higher BMI and TG values, as well as a higher rate of hyperlipidemia, than those with cirrhosis. Recent research indicates that the at-risk phenotype for HCC in NAFLD is primarily obese male patients with a history of diabetes and cardiovascular comorbidities [3]. This phenotype often overlaps with the profile

Table 3. Univariate and multivariate analyses of the associations between clinicopathologic characteristics and early washout (before 60 seconds) in hepatocellular carcinomas

Variable	Univariate analysis		Multivariate analysis	
	OR (95% CI)	P-value	OR (95% CI)	P-value
Age	0.996 (0.954–1.041)	0.875	–	–
Sex (male)	0.595 (0.178–1.993)	0.400	–	–
Body mass index	0.874 (0.740–1.034)	0.116	–	–
Platelets	0.999 (0.992–1.006)	0.853	–	–
International normalized ratio	0.001 (0.000–0.273)	0.018	0.002 (0.000–0.899)	0.046
Total bilirubin	0.557 (0.969–1.151)	0.360	–	–
Direct bilirubin	0.924 (0.808–1.399)	0.896	–	–
Albumin	0.147 (0.893–1.235)	0.586	–	–
Alanine transaminase	1.053 (0.986–1.021)	0.894	–	–
Aspartate transaminase	0.979 (0.988–1.025)	0.955	–	–
Alkaline phosphatase	0.594 (0.989–1.029)	0.537	–	–
Gamma-glutamyl transferase	1.268 (0.993–1.005)	0.440	–	–
Total cholesterol	1.074 (0.590–1.774)	0.952	–	–
Triglyceride	1.517 (0.369–1.900)	0.511	–	–
High-density lipoprotein	0.089 (1.404–99.132)	0.036	6.828 (0.652–71.541)	0.109
Low-density lipoprotein	1.558 (0.479–1.674)	0.595	–	–
Alpha-fetoprotein (positive)	0.533 (0.203–1.400)	0.202	–	–
Alpha-fetoprotein-L3 (positive)	0.679 (0.260–1.771)	0.428	–	–
PIVKA-II (positive)	0.870 (0.321–2.357)	0.784	–	–
microRNA (positive)	0.400 (0.112–1.422)	0.157	–	–
Tumor differentiation				
Well (n=9)	Reference		Reference	
Moderate (n=45)	9.143 (1.055–79.261)	0.045	7.259 (0.798–66.030)	0.078
Poor (n=18)	28.000 (2.651–295.718)	0.006	21.930 (1.960–245.319)	0.012
Hepatic steatosis grade				
S1 (n=35)	Reference			
S2 (n=19)	1.456 (0.472–4.491)	0.513	–	
S3 (n=18)	1.664 (0.523–5.289)	0.388	–	
Hepatic fibrosis stage				
F0 (n=11)	Reference			
F1 (n=4)	0.833 (0.084–8.240)	0.876	–	
F2 (n=24)	0.705 (0.168–2.955)	0.633	–	
F3 (n=33)	1.282 (0.324–5.081)	0.724	–	
Hepatic inflammation activity				
A0 (n=11)	Reference			
A1 (n=18)	1.042 (0.231–4.704)	0.958	–	–
A2 (n=38)	1.146 (0.297–4.421)	0.843	–	–
A3 (n=5)	0.208 (0.017–2.518)	0.217	–	–
Microvascular invasion				
M0 (n=55)	Reference			
M1 (n=14)	1.195 (0.366–3.904)	0.768	–	–
M2 (n=3)	1.793 (0.153–20.949)	0.641	–	–
Ki-67	0.530 (0.082–3.419)	0.505	–	–

OR, odds ratio; CI, confidence interval; PIVKA-II, protein induced by vitamin K absence or antagonist-II.

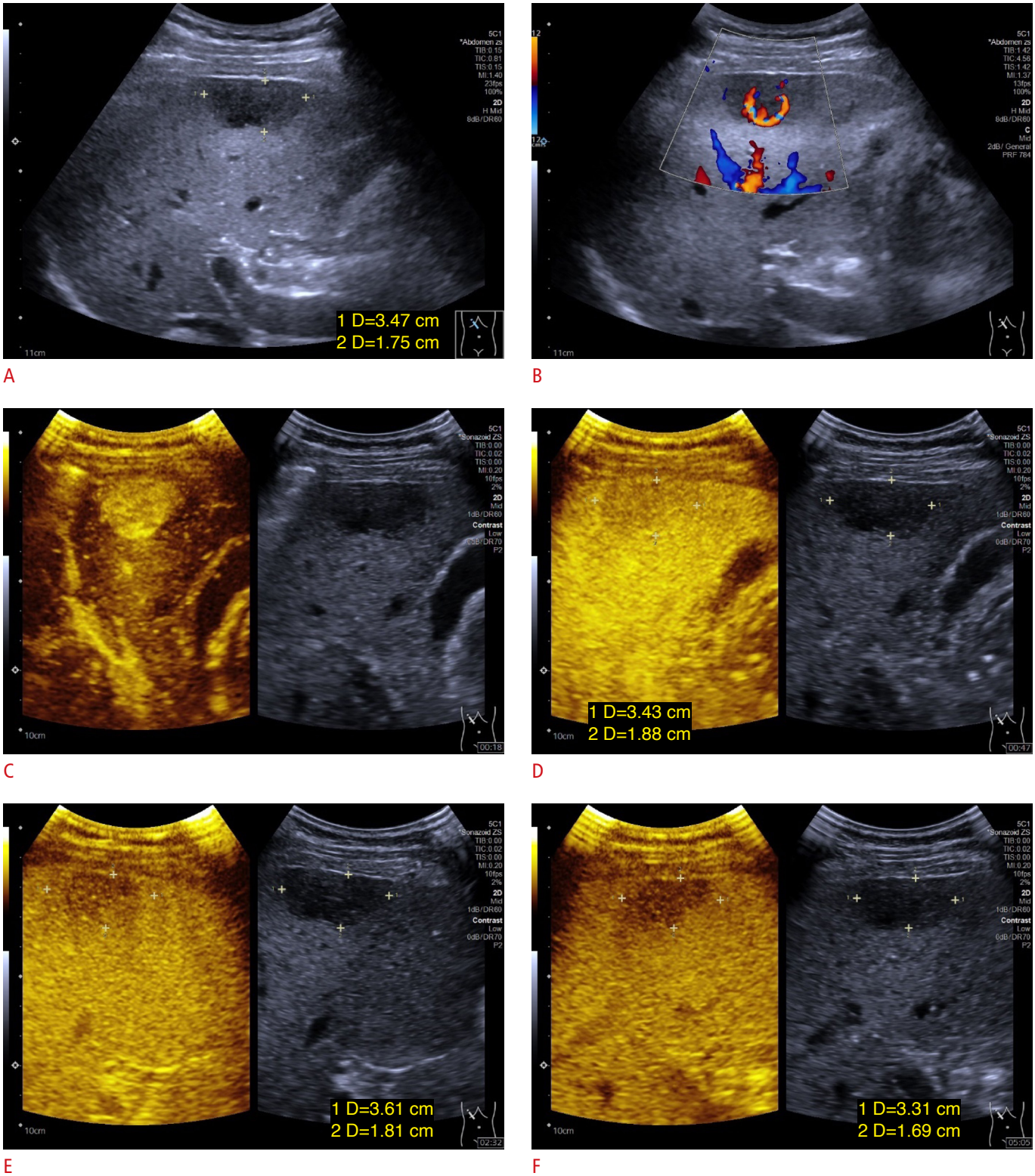

Fig. 1. A 57-year-old patient with an incidentally detected focal liver lesion in the right lobe of his liver.
A. A 35-mm hypoechoic mass with an ill-defined margin and irregular shape was evident against the background of fatty liver. B. Color flow signals were detected within the lesion, with a measured resistance index of 0.67. C–F. On contrast-enhanced ultrasound with Sonazoid, the lesion demonstrated hyperenhancement during the arterial phase (C), relatively early washout at approximately 50 seconds in the portal venous phase (D), and marked hypoenhancement in the later phase (E) and Kupffer phase (F). Surgical resection and histopathological evaluation confirmed the diagnosis of hepatocellular carcinoma (tumor differentiation, poor; hepatic steatosis grade, S1; hepatic fibrosis stage, F1).

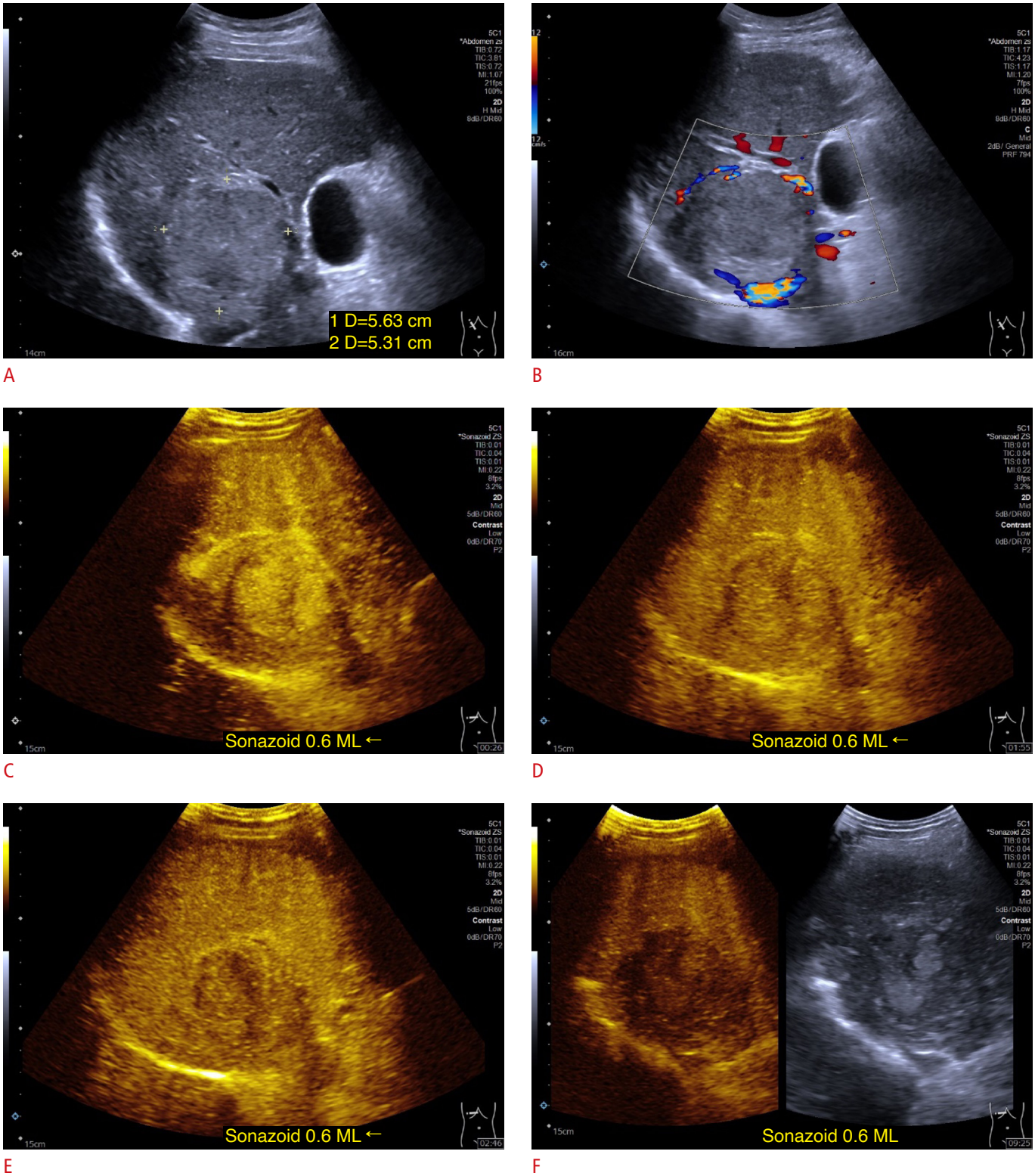

Fig. 2. A focal liver lesion in a 54-year-old male patient with cirrhosis.
A. A 56-mm hyperechoic lesion was detected in the right lobe of the liver. B. Color flow signals were observed around the lesion, with a measured resistance index of 0.65. C–F. Following the injection of Sonazoid, the lesion exhibited hyperenhancement during the arterial phase (C) and isoenhancement during the portal venous phase (D). The enhancement washed out after 120 seconds, and the lesion exhibited hypoenhancement in the late phase (E) and Kupffer phase (F). Surgical resection and subsequent histopathological examination confirmed the diagnosis of hepatocellular carcinoma (tumor differentiation, moderate; hepatic steatosis grade, S0; hepatic fibrosis stage, F4).

of patients with NAFLD who should be screened for NASH, as recommended by current European clinical practice guidelines [24]. Many patients remain undiagnosed and untreated because of the lack of generally accepted non-invasive methods and molecular markers to stratify HCC risk in the NAFLD population [25].

Conventional BMUS may display limited performance in patients with NAFLD due to ultrasound beam attenuation in a bright liver background and heterogeneously distributed focal fatty infiltration [3]. In the present study, the conventional ultrasound appearances of NAFLD-related HCCs resembled those of cirrhosis-related HCCs. Previous research has demonstrated that patients with HCC in non-cirrhotic livers tend to have larger nodules and/or higher recurrence rates compared with those with HCC in cirrhosis [26]. HCC growth in non-cirrhotic patients is often clinically silent in the early stages because of a lack of symptoms and preserved hepatic function [27]. However, the current study did not find significant differences in tumor size between NAFLD-related HCC in non-cirrhotic livers and cirrhosis-related HCC, suggesting that HCC size at diagnosis may vary according to local surveillance practices and other factors [28].

In both groups of this study, most HCC lesions exhibited hyperenhancement during the arterial phase on Sonazoid-CEUS. A key CEUS feature of HCC is that it receives a higher proportion of blood supply from the hepatic artery compared with the normal liver, which is predominantly supplied by the portal vein [29,30]. Poorly differentiated HCCs, particularly those with an infiltrative imaging appearance, may transition from aerobic to glycolytic metabolism, leading to reduced expression of angiogenic signaling pathways and possibly causing isoenhancement during the arterial phase [31]. One case of cirrhosis-related HCC displayed rim hyperenhancement, a feature most commonly observed in liver metastases, presumably related to marked fibrous stroma and central necrosis [32].

According to current WFUMB guidelines for CEUS in the liver, the key diagnostic criteria for HCC—arterial phase hyperenhancement followed by washout—were met [21,33]. The present findings demonstrated that NAFLD-related HCC exhibited earlier washout than HBV cirrhosis–related HCC. Approximately half of the NAFLD-related HCC lesions showed washout within 1 minute, which largely aligns with previous reports of HCC developing in non-cirrhotic livers [27,32,34]. Recent research has identified multiple factors associated with HCC washout time on CEUS, including tumor size and differentiation, the presence of MVI, and whether the tumor is primary or recurrent [35]. Histopathologically, diminished portal venous supply due to reduced or absent normal portal triad structures likely contributes to the early washout feature [29]. The current multivariate logistic regression analysis revealed that both INR and poor tumor differentiation were significantly correlated with washout times of less than 1 minute in NAFLD-related HCC. Because INR is related to liver function, higher Child-Pugh class, and poorer coagulation status [36], a normal or low INR is more common in NAFLD than in cirrhosis. Consequently, a low INR correlates with HCC in a non-cirrhotic liver background and early washout on Sonazoid-CEUS. A study by Myers et al. [37] showed that patients with NAFLD-related HCC had lower INR values compared with non-NAFLD cases, which is consistent with the present findings. Moreover, washout is observed more frequently in HCC with lower histopathologic grades or poorer differentiation [21]. Given that histopathological grade is a well-recognized predictor of recurrence and survival in patients with HCC, the correlation between poor differentiation and early washout in NAFLD-related HCC on Sonazoid-CEUS may have important implications for future treatment strategies [38].

A study by Thompson et al. [39] suggested that the imaging characteristics of NAFLD-related HCC may vary significantly across the NAFLD spectrum, depending on the degree of hepatic steatosis and the presence of cirrhosis. In the present study, both the NAFLD and HBV-related liver cirrhosis groups exhibited high rates of inflammation, which thus represents a potential risk factor for HCC. Accordingly, the correlations between hepatic steatosis grade and imaging features, such as the Kupffer phase hypoenhancement on Sonazoid-CEUS, may have potential applications in the detection and diagnosis of HCC in patients with NAFLD.

This study had several limitations. First, it was a retrospective single-center study with a relatively small sample size. Second, the term NAFLD is increasingly being replaced internationally by metabolic dysfunction-associated steatotic liver disease (MASLD) [4]. However, as the diagnoses of MASLD and NAFLD have been shown to correspond, the terms are often used interchangeably. Additionally, the selection of HBV as the sole etiology of liver cirrhosis for comparison warrants further justification in future studies.

In conclusion, NAFLD-related HCC demonstrates characteristic enhancement patterns on Sonazoid-enhanced CEUS, including hyperenhancement during the arterial phase followed by relatively early and marked washout. Furthermore, the Sonazoid-enhanced CEUS features of NAFLD-related HCC are associated with the clinicopathologic characteristics of INR, tumor differentiation, and hepatic steatosis grade.

ORCID: Yi Dong: https://orcid.org/0000-0002-0212-1477; Juan Cheng: https://orcid.org/0009-0005-5526-8455; Yun-Lin Huang: https://orcid.org/0000-0002-9373-3304; Yi-Jie Qiu: https://orcid.org/0000-0002-8837-6074; Jia-Ying Cao: https://orcid.org/0009-0006-9526-9441; Xiu-Yun Lu: https://orcid.org/0000-0002-6045-8027; Wen-Ping Wang: https://orcid.org/0000-0002-6797-1835; Kathleen Möller: https://orcid.org/0009-0002-9492-0141; Christoph F. Dietrich: https://orcid.org/0000-0001-6015-6347

Author Contributions

Conceptualization: Dong Y, Dietrich CF. Data acquisition: Cheng J, Qiu YJ, Möller K. Data analysis or interpretation: Huang YL, Cao JY, Lu XY, Wang WP. Drafting of the manuscript: Dong Y, Cheng J, Huang YL, Qiu YJ, Cao JY, Lu XY, Dietrich CF. Critical revision of the manuscript: Wang WP, Möller K, Dietrich CF. Approval of the final version of the manuscript: all authors.

Conflict of Interest

No potential conflict of interest relevant to this article was reported

References

1. Loomba R, Friedman SL, Shulman GI. Mechanisms and disease consequences of nonalcoholic fatty liver disease. Cell 2021;184:2537-2564.
2. Shah PA, Patil R, Harrison SA. NAFLD-related hepatocellular carcinoma: the growing challenge. Hepatology 2023;77:323-338.
3. Younes R, Bugianesi E. Should we undertake surveillance for HCC in patients with NAFLD? J Hepatol 2018;68:326-334.
4. Huang DQ, El-Serag HB, Loomba R. Global epidemiology of NAFLD-related HCC: trends, predictions, risk factors and prevention. Nat Rev Gastroenterol Hepatol 2021;18:223-238.
5. Singal AG, El-Serag HB. Rational HCC screening approaches for patients with NAFLD. J Hepatol 2022;76:195-201.
6. Lupsor-Platon M, Serban T, Silion AI, Tirpe GR, Tirpe A, Florea M. Performance of ultrasound techniques and the potential of artificial intelligence in the evaluation of hepatocellular carcinoma and non-alcoholic fatty liver disease. Cancers (Basel) 2021;13:790.
7. Jennison E, Patel J, Scorletti E, Byrne CD. Diagnosis and management of non-alcoholic fatty liver disease. Postgrad Med J 2019;95:314-322.
8. Hernaez R, Lazo M, Bonekamp S, Kamel I, Brancati FL, Guallar E, et al. Diagnostic accuracy and reliability of ultrasonography for the detection of fatty liver: a meta-analysis. Hepatology 2011;54:1082-1090.
9. Barr RG. Contrast enhanced ultrasound for focal liver lesions: how accurate is it? Abdom Radiol (NY) 2018;43:1128-1133.
10. Quaia E, Calliada F, Bertolotto M, Rossi S, Garioni L, Rosa L, et al. Characterization of focal liver lesions with contrast-specific US modes and a sulfur hexafluoride-filled microbubble contrast agent: diagnostic performance and confidence. Radiology 2004;232:420-430.
11. Dai Y, Chen MH, Yin SS, Yan K, Fan ZH, Wu W, et al. Focal liver lesions: can SonoVue-enhanced ultrasound be used to differentiate malignant from benign lesions? Invest Radiol 2007;42:596-603.
12. Schoenberger H, Chong N, Fetzer DT, Rich NE, Yokoo T, Khatri G, et al. Dynamic changes in ultrasound quality for hepatocellular carcinoma screening in patients with cirrhosis. Clin Gastroenterol Hepatol 2022;20:1561-1569.
13. Samoylova ML, Mehta N, Roberts JP, Yao FY. Predictors of ultrasound failure to detect hepatocellular carcinoma. Liver Transpl 2018;24:1171-1177.
14. Huang DQ, Fowler KJ, Liau J, Cunha GM, Louie AL, An JY, et al. Comparative efficacy of an optimal exam between ultrasound versus abbreviated MRI for HCC screening in NAFLD cirrhosis: a prospective study. Aliment Pharmacol Ther 2022;55:820-827.
15. Cocciolillo S, Parruti G, Marzio L. CEUS and Fibroscan in non-alcoholic fatty liver disease and non-alcoholic steatohepatitis. World J Hepatol 2014;6:496-503.
16. Dong Y, Zuo D, Qiu YJ, Cao JY, Wang HZ, Wang WP. Prediction of histological grades and Ki-67 expression of hepatocellular carcinoma based on sonazoid contrast enhanced ultrasound radiomics signatures. Diagnostics (Basel) 2022;12:2175.
17. Kudo M. Defect reperfusion imaging with Sonazoid(R): a breakthrough in hepatocellular carcinoma. Liver Cancer 2016;5:1-7.
18. Barr RG, Huang P, Luo Y, Xie X, Zheng R, Yan K, et al. Contrast-enhanced ultrasound imaging of the liver: a review of the clinical evidence for SonoVue and Sonazoid. Abdom Radiol (NY) 2020;45:3779-3788.
19. Chen S, Qiu YJ, Zuo D, Shi SN, Wang WP, Dong Y. Imaging features of hepatocellular carcinoma in the non-cirrhotic liver with Sonazoid-enhanced contrast-enhanced ultrasound. Diagnostics (Basel) 2022;12:2272.
20. Lee JY, Minami Y, Choi BI, Lee WJ, Chou YH, Jeong WK, et al. The AFSUMB consensus statements and recommendations for the clinical practice of contrast-enhanced ultrasound using Sonazoid. Ultrasonography 2020;39:191-220.
21. Dietrich CF, Nolsoe CP, Barr RG, Berzigotti A, Burns PN, Cantisani V, et al. Guidelines and good clinical practice recommendations for contrast-enhanced ultrasound (CEUS) in the liver-update 2020 WFUMB in cooperation with EFSUMB, AFSUMB, AIUM, and FLAUS. Ultrasound Med Biol 2020;46:2579-2604.
22. Bedossa P, Poynard T. An algorithm for the grading of activity in chronic hepatitis C: the METAVIR Cooperative Study Group. Hepatology 1996;24:289-293.
23. Yao J, Li K, Yang H, Lu S, Ding H, Luo Y, et al. Analysis of Sonazoid contrast-enhanced ultrasound for predicting the risk of microvascular invasion in hepatocellular carcinoma: a prospective multicenter study. Eur Radiol 2023;33:7066-7076.
24. European Association for the Study of the Liver; European Association for the Study of Diabetes; European Association for the Study of Obesity. EASL-EASD-EASO Clinical Practice Guidelines for the management of non-alcoholic fatty liver disease. J Hepatol 2016;64:1388-1402.
25. Heimbach JK, Kulik LM, Finn RS, Sirlin CB, Abecassis MM, Roberts

LR, et al. AASLD guidelines for the treatment of hepatocellular carcinoma. Hepatology 2018;67:358-380.
26. Mohamad B, Shah V, Onyshchenko M, Elshamy M, Aucejo F, Lopez R, et al. Characterization of hepatocellular carcinoma (HCC) in non-alcoholic fatty liver disease (NAFLD) patients without cirrhosis. Hepatol Int 2016;10:632-639.
27. Dong Y, Wang WP, Lee WJ, Meloni MF, Clevert DA, Chammas MC, et al. Contrast-enhanced ultrasound features of histopathologically proven hepatocellular carcinoma in the non-cirrhotic liver: a multicenter study. Ultrasound Med Biol 2022;48:1797-1805.
28. Al-Sharhan F, Dohan A, Barat M, Feddal A, Terris B, Pol S, et al. MRI presentation of hepatocellular carcinoma in non-alcoholic steatohepatitis (NASH). Eur J Radiol 2019;119:108648.
29. Narsinh KH, Cui J, Papadatos D, Sirlin CB, Santillan CS. Hepatocarcinogenesis and LI-RADS. Abdom Radiol (NY) 2018;43:158-168.
30. Kim CK, Lim JH, Park CK, Choi D, Lim HK, Lee WJ. Neoangiogenesis and sinusoidal capillarization in hepatocellular carcinoma: correlation between dynamic CT and density of tumor microvessels. Radiology 2005;237:529-534.
31. Pei XQ, Liu LZ, Zheng W, Cai MY, Han F, He JH, et al. Contrast-enhanced ultrasonography of hepatocellular carcinoma: correlation between quantitative parameters and arteries in neoangiogenesis or sinusoidal capillarization. Eur J Radiol 2012;81:e182-e188.
32. Dong Y, Chen S, Moller K, Qiu YJ, Lu XY, Zhang Q, et al. Applications of dynamic contrast-enhanced ultrasound in differential diagnosis of hepatocellular carcinoma and intrahepatic cholangiocarcinoma in non-cirrhotic liver. Ultrasound Med Biol 2023;49:1780-1788.
33. Wang JY, Feng SY, Yi AJ, Zhu D, Xu JW, Li J, et al. Comparison of contrast-enhanced ultrasound versus contrast-enhanced magnetic resonance imaging for the diagnosis of focal liver lesions using the Liver Imaging Reporting and Data System. Ultrasound Med Biol 2020;46:1216-1223.
34. Chen S, Qiu YJ, Zuo D, Shi SN, Wang WP, Dong Y. Imaging features of hepatocellular carcinoma in the non-cirrhotic liver with Sonazoid-enhanced contrast-enhanced ultrasound. Diagnostics (Basel) 2022;12:2272.
35. Fan PL, Ding H, Mao F, Chen LL, Dong Y, Wang WP. Enhancement patterns of small hepatocellular carcinoma (≤ 30 mm) on contrast-enhanced ultrasound: correlation with clinicopathologic characteristics. Eur J Radiol 2020;132:109341.
36. Kalas MA, Chavez L, Leon M, Taweesedt PT, Surani S. Abnormal liver enzymes: a review for clinicians. World J Hepatol 2021;13:1688-1698.
37. Myers S, Neyroud-Caspar I, Spahr L, Gkouvatsos K, Fournier E, Giostra E, et al. NAFLD and MAFLD as emerging causes of HCC: a populational study. JHEP Rep 2021;3:100231.
38. Qin X, Hu X, Xiao W, Zhu C, Ma Q, Zhang C. Preoperative evaluation of hepatocellular carcinoma differentiation using contrast-enhanced ultrasound-based deep-learning radiomics model. J Hepatocell Carcinoma 2023;10:157-168.
39. Thompson SM, Garg I, Ehman EC, Sheedy SP, Bookwalter CA, Carter RE, et al. Non-alcoholic fatty liver disease-associated hepatocellular carcinoma: effect of hepatic steatosis on major hepatocellular carcinoma features at MRI. Br J Radiol 2018;91:20180345.